JOURNAL OF VIROLOGY, Oct. 1995, p. 6090–6097 Vol. 69, No. 10
0022-538X/95/$04.00+0

Concerted Integration of Retrovirus-Like DNA by Human Immunodeficiency Virus Type 1 Integrase

GOODARZ GOODARZI,[1] GUANG-JIN IM,[1] KARL BRACKMANN,[2] AND DUANE GRANDGENETT[1]*

St. Louis University Health Science Center, Institute for Molecular Virology, St. Louis, Missouri 63110,[1] and Genetics Systems Corporation, Redmond, Washington 98052-5039[2]

Received 21 February 1995/Accepted 26 June 1995

The integration of linear retrovirus DNA by the viral integrase (IN) into the host chromosome occurs by a concerted mechanism (full-site reaction). IN purified from avian myeloblastosis virus and using retrovirus-like DNA restriction fragments (487 bp in length) as donors and circular DNA (pGEM-3) as the target can efficiently catalyze that reaction. Nonionic detergent lysates of purified human immunodeficiency virus type 1 (HIV-1) virions were also capable of catalyzing the concerted integration reaction. The donor substrates were restriction fragments (469 bp) containing either U3-U5 (H-2 donor) or U5-U5 (H-5 donor) long terminal repeat sequences at their ends. As was shown previously with bacterially expressed HIV-1 IN, the U5 terminus of H-2 was preferred over the U3 terminus by virion-associated IN. The reactions involving two donors per circular target by HIV-1 IN preferred Mg^{2+} over Mn^{2+}. Both metal ions were equally effective for the circular half-site reaction involving only one donor molecule. The linear 3.8-kbp recombinant products produced from two donor insertions into pGEM were genetically selected, and the donor-target junctions of individual recombinants were sequenced. A total of 55% of the 87 sequenced recombinants had host site duplications of between 5 and 7 bp, with the HIV-1 5-bp-specific duplication predominating. The other recombinants that migrated at the linear 3.8-kbp position were mainly small deletions that were grouped into four sets of 17, 27, 40, and 47 bp, each having a periodicity mimicking a turn of the DNA helix. Aprotic solvents (dimethyl sulfoxide and 1,4-dioxane) enhanced both the half-site and the linear 3.8-kbp strand transfer reactions which favored low-salt conditions (30 mM NaCl). The order of addition of the donor and target during preincubation with HIV-1 IN on ice did not affect the quantity of linear 3.8-kbp recombinants relative to that of the circular half-site products that were produced; only the quantity of donor-donor versus donor-target recombinants was affected. The presence of Mg^{2+} in the preincubation mixtures containing donor and target substrates was not necessary for the stability of preintegration complexes on ice or at 22°C. Comparisons of the avian and HIV-1 concerted integration reactions are discussed.

Efficient replication of retroviruses is dependent upon the integration of the viral DNA genome into the host DNA (18, 25, 29). The viral integrase (IN) catalyzes both the 3′ OH trimming reaction on the blunt-ended linear viral DNA and the concerted integration of the recessed DNA into the chromosomal DNA (2, 3, 14, 17, 26). IN is associated with the viral DNA in high-molecular-weight nucleoprotein complexes found in virus-infected cells (1, 2, 14, 15, 24, 26). The reported sizes of the nucleoprotein complexes differ, running between ~80S for human immunodeficiency virus type 1 (HIV-1) and ~160S for murine leukemia virus.

The mechanisms involved in the nuclear transport of these nucleoprotein complexes have been investigated. An active transport mechanism that requires ATP but does not depend on cell division allows the HIV-1 nucleoprotein complexes to be transported from the cytoplasm to the nucleus (4, 5, 20). The nuclear targeting of the HIV-1 complex is dependent on the viral matrix and Vpr proteins, while the murine leukemia virus complex requires the dissolution of the nuclear envelope during mitosis (5, 20, 21, 27). The viral protein composition of the nucleoprotein complexes appears to vary, depending on the isolation procedures used with HIV-1 (1, 6, 15, 21).

In vitro integration systems using purified IN and retrovirus-like donor DNAs are potential tools to investigate the molecular mechanisms involved in the assembly, stability, and catalytic properties of viral nucleoprotein complexes. IN from bacterial expression systems or purified from avian myeloblastosis virus (AMV) has been coupled with the use of oligonucleotides containing viral DNA terminal sequences to investigate both the 3′ OH trimming and half-site strand transfer reactions (7, 8, 10, 13, 15, 19, 22, 23, 28, 32, 33). The assembly process for forming nucleoprotein complexes in vitro or preintegration complexes capable of performing the strand transfer reactions has been investigated (9, 11, 16, 34, 35). Recent studies using IN purified from AMV have shown that the concerted integration (or full-site) reaction using a retrovirus-like DNA donor (termed M-2) is efficiently catalyzed by the virion-derived protein (34, 35). The recessed viral termini of two individual donors (each 487 bp in length) were efficiently paired by AMV IN in preintegration complexes that were capable of catalyzing the concerted integration of the donors into circular target DNA. Baculovirus-expressed HIV-1 IN is capable of performing the full-site reaction but was quite inefficient (8). Bacterially expressed HIV-1 IN and feline retrovirus IN also appear to lack the ability to perform the concerted integration involving the pairing of two viral DNA ends into exogenous DNA targets (12, 31).

We wanted to investigate the molecular mechanisms and the efficiency of the full-site integration reaction catalyzed by IN activity derived from HIV-1 virion lysates. We constructed two linear virus-like DNA donors (Fig. 1A) similar in size to that of

* Corresponding author. Mailing address: Institute for Molecular Virology, 3681 Park Ave., St. Louis, MO 63110. Phone: (314) 577-8411. Fax: (314) 577-8406. Electronic mail address: Grandgdp@SLUVCA.SLU.EDU.

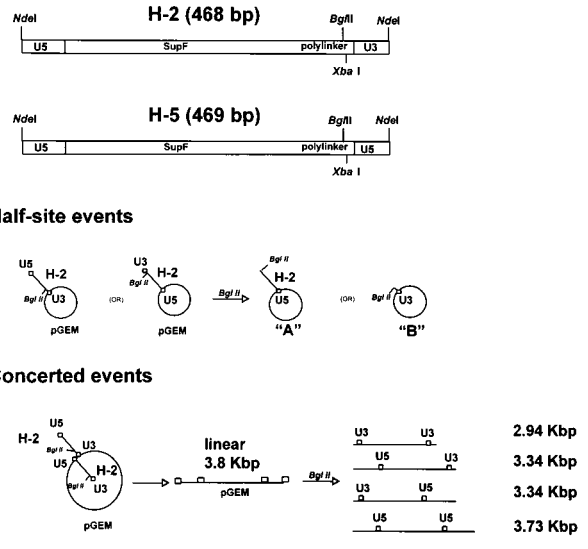

FIG. 1. DNA structures and pathways involved in half-site and concerted integration events catalyzed by HIV-1 IN. (A) The H-2 donor possesses the terminal 20 bp of the U3 and U5 HIV-1 LTR termini. The H-5 donor contains only U5 LTR termini. Both constructs are flanked by *Nde*I sites. The *supF* gene and various restriction enzyme sites are also shown. (B) Half-site insertion of H-2 into circular target DNA (pGEM) by IN. *Bgl*II digestion of half-site recombinants produces two different ball-and-stick molecules ("A" and "B"), depending on which terminus is inserted. The same pattern is observed with H-5. (C) The concerted or adjacent integration of two separate H-2 molecules into pGEM produces a linear 3.8-kbp DNA. Four different recombinants are possible, depending on the frequency of U3 or U5 insertions. *Bgl*II digestion of the 3.8-kbp DNA results in the formation of four linear structures, with the two 3.34-kbp structures comigrating.

the avian system (34, 35). The H-2 and H-5 donors contained recessed 3′ OH ends and the *supF* gene for the genetic selection of individual donor-target recombinants for DNA sequence analysis. The H-2 ends were composed of HIV-1 U3 and U5 long terminal repeat (LTR) termini, and the H-5 ends contained only U5 LTR sequences. The U5 terminus is highly preferred by bacterially expressed HIV-1 IN for both the 3′ OH trimming and half-site strand transfer reactions (13, 30, 32).

The ability of IN found in HIV-1 virion lysates to integrate either the H-2 or H-5 donors into circular pGEM DNA was investigated under a variety of assay conditions. Various parameters, such as the donor-target ratio, protein concentration, aprotic solvents, and NaCl concentrations, were analyzed. Divalent metal ions (Mg^{2+} and Mn^{2+}) that govern the efficiency of full-site reactions were also investigated. The H-2–pGEM and H-5–pGEM recombinants were characterized by agarose gel electrophoresis, restriction enzyme digestion, and dideoxy DNA sequencing of the donor-target junctions of individually isolated recombinants. In an effort to elucidate the nature of preintegration complex formation observed with virion lysates, the assembly and stability of IN–H-5–pGEM complexes were examined by order-of-addition experiments and under different preincubation conditions.

MATERIALS AND METHODS

Bacteria, plasmids, and oligonucleotides. *Escherichia coli* (strain CA244) that has amber mutations in the *lacZ* gene and mutations for tryptophan biosynthesis was obtained from the *E. coli* Genetic Stock Center at Yale University. CA244 cells were transformed with H-2–pGEM and H-5–pGEM recombinants that were derived from the ligation of isolated linear 3.8-kbp DNA. Transformed colonies were isolated as previously described (35). Plasmids pUC19 and pGEM-3 were acquired from Promega. Oligonucleotides that made up the U3-U5 (H-2) and the U5-U5 (H-5) LTR constructs contained an internal *Eco*RI site and terminal *Nde*I sites (Operon Technologies, Inc.).

Construction of H-2 and H-5 donor substrates. The U3-U5 and U5-U5 oligonucleotides were cloned into the *Nde*I site of a pUC19 plasmid whose *Eco*RI site was destroyed by a Klenow DNA polymerase fill-in reaction. The constructs containing the individual oligonucleotides were linearized by *Eco*RI digestion. A fragment containing the *supF* gene was cloned in the *Eco*RI site by blunt-end ligation. The H-2 and H-5 donors were sequenced. Digestion of the new constructs with *Nde*I yielded a 468-bp restriction fragment for H-2 that contained the U5 and U3 LTR termini and a 469-bp restriction fragment for H-5 that contained the two U5 LTR termini (Fig. 1A).

Labeling of H-2 and H-5 donor substrates. Supercoiled pUC19 plasmids containing H-2 or H-5 were isolated by velocity sedimentation on sucrose gradients. The H-2 or H-5 donor fragments were released from pUC19 by *Nde*I digestion and isolated from low-melting-point agarose gels. Both donors were dephosphorylated and 5′ end labeled with [γ-^{32}P]ATP and T4 polynucleotide kinase. The specific activities of these constructs were between 10,000 and 20,000 cpm/ng of DNA. The target, supercoiled pGEM, was also isolated on sucrose gradients.

Virus and enzymes. HIV-1 (LAV strain) was purified by equilibrium sedimentation on sucrose gradients and concentrated by pelleting onto sucrose cushions. The LAV virus was harvested from virus-infected CEM cells. The HIV-1 virus was suspended in a buffer containing 10 mM Tris-HCl, 0.1 M NaCl, and 0.1 mM EDTA. The viral protein concentration was between 3 and 5 mg/ml. The standard concentration of viral protein for lysis was 0.3 mg/ml. Unless otherwise stated, the virus was lysed on ice for 5 min in a buffer consisting of 0.05 M NaCl, 25 mM HEPES (*N*-2-hydroxyethylpiperazine-*N*′-2-ethanesulfonic acid) (pH 7.6), 0.1% Triton X-100, and 1 mM dithiothreitol. For high-salt lysis buffer experiments, 0.3 M NaCl was used.

T4 polynucleotide kinase, T4 DNA ligase, restriction endonucleases, and exonuclease-free Klenow DNA polymerase were purchased from Promega. The Sequenase kit obtained from U.S. Biochemicals was used for DNA sequencing.

Assay conditions. The standard reaction mixture contained 20 mM HEPES (pH 7.6), 5 mM dithiothreitol, 10 mM $MgCl_2$, 12% dimethyl sulfoxide (DMSO), 5% polyethylene glycol (PEG), and NaCl at between 30 and 60 mM. The preincubation step included the mixing of donor DNA (H-2 or H-5), pGEM, and lysed virions on ice for 12 min in 25-μl aliquots. The protein concentration was usually between 1 and 2.5 μg per assay. The strand transfer reactions were at 37°C. Times of incubation were between 15 and 45 min. The concentrations of H-2 or H-5 and pGEM were 60 and 100 ng per assay, respectively. The molar ratio of donor to pGEM was 4 to 1, respectively. For the scaled-up reactions, the same concentrations of viral protein lysate and DNA substrates were maintained for the isolation of various H-2–pGEM and H-5–pGEM concerted or linear 3.8-kbp recombinants.

Analysis of H-2–pGEM and H-5–pGEM recombinants. The reactions were stopped with sodium dodecyl sulfate (SDS) and proteinase K at final concentrations of 1% and 1 mg/ml, respectively. The samples were further incubated at 37°C for 1 h. The DNA products were subjected to phenol-chloroform extractions and ethanol precipitation. Aliquots were analyzed on 1% agarose gels with a Tris-borate-EDTA buffer. The gels were dried and exposed to X-ray films. The products were quantitated with a Molecular Dynamics PhosphorImager. For *Bgl*II restriction analysis, each 25-μl reaction sample was digested with 12 U of *Bgl*II for 2 h. The samples were subjected to electrophoresis on 1.5% agarose gels for 13 h at 105 V. The gels were stained with ethidium bromide. A linear 3.34-kbp DNA marker was 5′ end labeled with [γ-^{32}P]ATP to identify the linear 3.34-kbp DNA obtained by *Bgl*II digestion of H-2–pGEM and H-5–pGEM recombinants. Linear DNA fragments (Boehringer Mannheim), linear and nicked circular pGEM, and a linear and nicked circular 3.34-kbp marker (35) were used as unlabeled molecular weight markers.

Sequencing of H-2–pGEM and H-5–pGEM recombinants. The linear 3.8-kbp DNA obtained from either H-2–pGEM or H-5–pGEM recombinants that were the result of two donor reactions (Fig. 1C) was isolated with scaled-up reaction mixtures. The products were subjected to electrophoresis on 1.5% agarose gels, and the wet gels were exposed to X-ray film. The desired DNA was excised, electroeluted, and purified by Wizard PCR prep columns (Promega). The DNA was ligated and transformed into CA244 cells. Colonies were screened for plasmids, which were analyzed by size and restriction enzyme digestion. The appropriate plasmids were digested with *Sfu*I to remove one-half of each donor molecule from the 3.8-kbp recombinant. This removal permitted direct sequencing of the donor-target junctions located in the larger DNA fragment which was purified and eluted from agarose gels. The sequencing was accomplished by the dideoxy sequencing method. Primers for sequencing were homologous within the donors near both termini and were used to sequence the donor-target junction.

RESULTS

Optimization of virion lysis for production of H-2–pGEM and H-5–pGEM recombinants. We first established what solution conditions were best for nonionic detergent lysis of purified HIV-1 virions to produce strand transfer products.

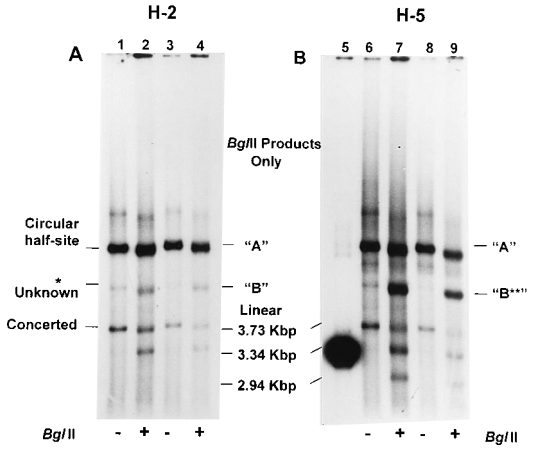

FIG. 2. Analysis of donor-target recombinants produced with H-2 or H-5 donors, the target, and virion-associated HIV-1 IN. H-2 or H-5 and pGEM were preincubated with virions lysed with the 0.3 M NaCl lysis buffer and assayed under standard reaction conditions, using 60 mM NaCl. The reaction mixtures were incubated at 37°C for 20 min. The samples were processed, and some were (+) or were not (−) digested with *Bgl*II. The DNAs were subjected to electrophoresis on 1.5% agarose gels. The dried gels were exposed for 18 h without a screen. The H-2 and H-5 recombinants are shown in panels A and B, respectively. The right side of each gel shows *Bgl*II-digested products (Fig. 1), and the extreme left side indicates the undigested products for both gels. Lanes 1, 2, 6, and 7 and 3, 4, 8, and 9 contained 2.3 and 4.6 μg of viral protein, respectively. Lane 5 contained a labeled 3.4-kbp DNA marker. The asterisk identifies an unknown DNA recombinant structure that was also observed in Fig. 3 to 7. "B**" denotes the short-arm U5 insertions into pGEM that occurs with H-5 (Fig. 1).

The protein concentration of the virions was held constant at 300 μg/ml. The optimal NaCl concentration in the lysis buffer for strand transfer activity was between 30 and 50 mM (data not shown). As indicated earlier, a higher NaCl concentration (300 mM) was used for lysis in several experiments. The lysis was usually for 5 min on ice, but similar results were obtained when the lysis time was 1 min. Triton X-100 or Nonidet P-40 at 0.1% in the lysis buffer gave similar results. Typically, 5 μl of the lysed virions was transferred to the on-ice preincubation mixture (20 μl). The preincubation mixture containing the lysed virions, the H-2 or H-5 DNA donors, and the pGEM target was incubated on ice for 12 min prior to the strand transfer reaction. Further preincubation at 22°C for 5 min prior to strand transfer did not increase the production of either half-site or full-site H-5–pGEM recombinants (see Fig. 7). The samples were incubated at 37°C to initiate the strand transfer reaction, and the DNA recombinant products were examined on 1 or 1.5% agarose gels (see Fig. 2 to 7).

Structural characterization of circular half-site and linear 3.8-kbp H-2–pGEM and H-5–pGEM recombinants. The linear H-2 donor had recessed 3′ OH termini composed of HIV-1 LTR U3 and U5 sequences, while the H-5 donor contained only U5 sequences (Fig. 1A). IN from lysed virions, H-2 or H-5, and pGEM were preincubated together on ice for 12 min in the presence of Mg^{2+} prior to incubation at 37°C. The DNA samples were processed and subjected to gel electrophoresis on a 1.5% agarose gel for 13 h (Fig. 2). Concerted or linear 3.8-kbp recombinants resulting from adjacent integration events involving two individual H-2 or H-5 molecules into circular pGEM were observed (Fig. 1C; 2A, lanes 1 and 3; and 2B, lanes 6 and 8) (35). Circular half-site H-2–pGEM or H-5–pGEM recombinants that migrated at the nicked circle 3.34-kbp position were also produced (Fig. 1B and 2, lanes 1, 3, 6, and 8) (35). The majority of the circular half-site recombinants were probably stick-and-ball structures resulting from half-site integration of one H-2 or H-5 donor into pGEM as previously demonstrated by electron microscopy of similar structures produced by the avian system (35). Two other minor H-2–pGEM or H-5–pGEM recombinants were also observed, as shown in Fig. 2 (lanes 1, 3, 6, and 8). The recombinants that migrated more slowly than the circular half-site products were pGEM with two or more independent H-2 or H-5 inserts (35). The structure of the recombinants, identified with an asterisk in Fig. 2 and 3 and which migrated slightly faster than the circular half-site recombinants, is unknown.

*Bgl*II digestion of circular half-site H-2–pGEM and H-5–pGEM recombinants resulted in the production of circular pGEM with either a long arm ("A") or a short arm ("B" or "B**") (Fig. 2, lanes 2, 4, 7, and 9) (35). *Bgl*II digestion of the H-2–pGEM recombinants confirmed earlier data on the preference for U5 over U3 termini by HIV-1 IN (12, 30). Digestion of the half-site H-2–pGEM recombinants produced mainly "A" structures (Fig. 1B) containing only U5 inserts (Fig. 2A, lanes 2 and 4), while digestion of H-5–pGEM recombinants produced equal amounts of "A" and "B**" structures (Fig. 2B, lanes 7 and 9). Digestion of H-2 or H-5 linear 3.8-kbp recombinants with *Bgl*II produced three linear molecules with calculated and measured lengths of 2.94, 3.34, and 3.73 kbp (Fig. 2, lanes 2, 4, 7, and 9) (35). Similar analyses of U3 and U5 termini usage by HIV-1 IN can also be applied to the digestion of the linear 3.8-kbp recombinants (Fig. 1C; 2, lanes 2 and 7; and 3).

To affirm the origins of the *Bgl*II products produced by the digestion of the total product mixture, the three individual H-5–pGEM products were isolated (Fig. 3). The DNAs were digested with *Bgl*II and subjected to 1.4% agarose gel electrophoresis for 14 h. The circular half-site product gave rise to "A" and "B" type structures (Fig. 3, lanes 2 and 3). The linear 3.8-kbp product gave rise to the expected three linear products (Fig. 3, lanes 6 and 7). The linear 3.8-kbp product (Fig. 3, lane 9) was ligated, resulting in a circular molecule (lane 10) that was larger than the circular half-site product (lane 2). The unknown recombinant (Fig. 3, lane 4) gave rise to the three linear size products expected from *Bgl*II digestion of the linear 3.8-kbp product (lane 5). The data suggest that the unknown donor-target recombinant possesses a stable structure different from that of the linear 3.8-kbp DNA but contains the entire

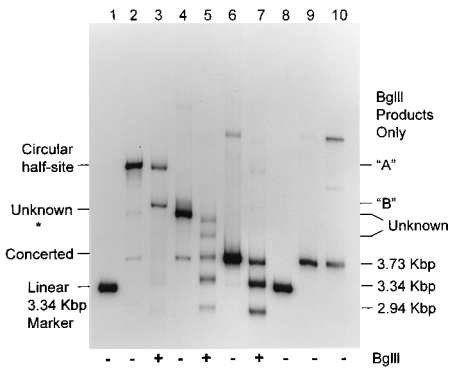

FIG. 3. *Bgl*II analysis of purified donor-target recombinants. The circular half-site, unknown, and linear 3.8-kbp H-5–pGEM recombinants were purified from 1.4% agarose gels, and the DNAs were digested with *Bgl*II. Lane 1, linear 3.34-kbp marker; lane 2, 12,500 cpm of undigested circular half-site DNA; lane 3, 12,500 cpm of circular half-site DNA digested with *Bgl*II; lane 4, 13,000 cpm of unknown DNA; lane 5, 13,000 cpm of unknown DNA digested with *Bgl*II; lane 6, 21,000 cpm of linear 3.8-kbp DNA; lane 7, 21,000 cpm of *Bgl*II-digested linear 3.8-kbp DNA; lane 8, linear 3.34-kbp marker; lanes 9 and 10, unligated and ligated linear 3.8-kbp DNA, respectively.

TABLE 1. Summary of concerted integration and deletion events with H-2 and H-5 donors[a]

Expt no. (donor)	No. of duplications by size (bp)						No. of deletions by size (bp)[b]				
	5	6	7	3	2	1	17–20	27–29	40	47–51	59 or 93
1 (H-5)	21	4	2	1	2	2	6	8	1	8	1
2 (H-2)	11	0	0	0	3	0	2	0	0	0	0
3 (H-5)	11	0	0	0	1	0	1	1	0	0	1
Total	43	4	2	1	6	2	9	9	1	8	2

[a] The full-site integration products were composed of different host duplication site types, with the HIV-specific (5-bp) duplication dominating. Three independent reactions were performed as indicated.

[b] The H-2 and H-5 donor sets had other integration events resulting in a majority of small deletions having periodicities of ~10 bp. No deletions smaller than 17 bp were observed. Two deletions are not shown: one 553-bp deletion in experiment 1 and one 580-bp deletion in experiment 2.

structure resulting from adjacent or concerted integration events (Table 1). Two other bands resulting from *Bgl*II digestion of the unknown recombinant were also observed (Fig. 3, lanes 4 and 5).

The purified linear 3.8-kbp DNA observed in Fig. 3 (lane 6) was examined by electron microscopy. The linear DNA was 3.77 kbp ± 100 bp in length and represented 96% of the recombinant DNA molecules observed in the sample (data not shown) (35).

Genetic selection and DNA sequence analysis of the concerted or linear 3.8-kbp H-2–pGEM and H-5–pGEM recombinants. To establish that some or all of the linear 3.8-kbp H-2–pGEM and H-5–pGEM recombinants were the result of full-site integration events, three independent scaled-up reactions were performed. The linear 3.8-kbp recombinant DNAs were isolated from wet 1.5% agarose gels and purified. The DNAs were ligated and transformed into *E. coli* CA244 cells (34, 35). In experiment 1, the virions were lysed at 50 mM NaCl and the strand transfer reaction was at 30 mM NaCl. A total of 56 colonies were isolated, and all of the plasmids were sequenced (Table 1). The HIV-1 5-bp host site duplication was predominant. Interestingly, the mainly small deletions generated by half-site integration events had a periodicity of approximately 10 bp. No deletions smaller than 17 bp were observed. The majority (~70%) of the deletions in each deletion series were 17, 27, and 49 bp in length. In experiments 2 and 3, the virions were lysed with 300 mM NaCl present and the reactions were at 60 mM NaCl. A total of 45 colonies were isolated, and 33 were sequenced. Again, the HIV-1 5-bp host site duplication was the major species observed. The number of deletions in experiments 2 and 3 were decreased compared with that in 1, but they were of the same size. The other 12 plasmids were characterized only by *Nde*I and *Bgl*II digestions. Their digestion patterns suggested that these plasmids were due to adjacent insertions of two donors into pGEM. In all three experiments, the duplication and deletion events mapped mainly between nucleotides 2070 through the polylinker site to 330 of pGEM-3 (data not shown) (34, 35). Two deletions and two duplications mapped to the same nucleotide position.

Solution conditions affect the circular half-site and the concerted or linear 3.8-kbp integration reactions. Solution conditions greatly influenced the concerted integration of the donor M-2 into pGEM, during which purified AMV IN was used for IN activity (34, 35). We investigated the effect of these same solution conditions on the strand transfer reaction catalyzed by HIV-1 IN. They included NaCl concentration, order of addition of donor and target substrates, donor-to-target ratios, protein concentration, and the presence of aprotic solvents (DMSO and dioxane) and PEG. The concentration of NaCl significantly affected both the concerted or linear 3.8-kbp and the circular half-site strand transfer reactions catalyzed by IN found in lysed HIV-1 virions (Fig. 4, lanes 2 to 10). All of the strand transfer reactions were proportionally decreased, including the donor-donor (H-5–H-5) recombinants, with increased concentrations of NaCl in the preincubation mixture prior to catalysis at the same salt concentration. The same decreases in strand transfer activity were observed when the preincubation step was at 30 mM NaCl but catalysis was at 70 or 100 mM (data not shown). The products that migrated slightly more slowly than the H-5–H-5 recombinants probably represented recombinants containing three donor molecules resulting from half-site reaction events (Fig. 4, lanes 2 to 4). On the basis of PhosphorImager data, the total decrease of all strand transfer products between the 30 mM NaCl set and the 70 mM set was 70 to 85%. In the 30 mM set, the total amount of H-5 integrated into all of the strand transfer products was between 4.5 to 6% of the input donor.

The order of addition of donor and target substrates to the preincubation mixture differentially affected the total quantities of H-5–pGEM recombinants that were produced compared with those of the H-5–H-5 recombinants (Fig. 4). But the total quantities of all recombinants that were produced in each reaction were similar (Fig. 4, lanes 2 to 4). With H-5 only in the preincubation mixture, 71% of the products were donor-donor recombinants (Fig. 4, lane 3). With pGEM only in the preincubation mixture, 34% of the products were donor-donor recombinants (Fig. 4, lane 4). With H-5 and pGEM present in the mixture, there was an equal distribution of strand transfer products between donor-donor and donor-pGEM products (Fig. 4, lane 2). The ratio of the circular half-site to the concerted or linear 3.8-kbp products that were produced (~4 to 1, respectively) held constant for the three different order-of-addition experiments (Fig. 4, lanes 2 to 4). These results suggest that the products which are formed in the reaction mixture

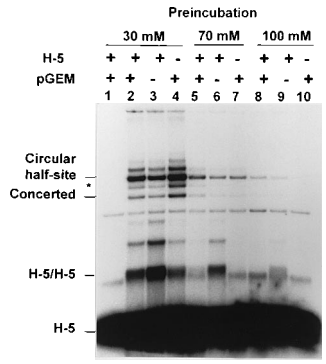

FIG. 4. Patterns of H-5–pGEM recombinants produced at various NaCl concentrations and different order-of-addition conditions. Standard reaction conditions were employed, except for the presence or absence of IN, H-5, and pGEM in the preincubation mixture. The top lines indicate which reagents were present (+) or not (−) in the preincubation mixture. The reactions were initiated by the addition of H-5 or pGEM as needed. The strand transfer reaction mixture was incubated at 37°C for 15 min. The NaCl concentrations are identified for each set of reactions. Lane 1 contained no virus. Depending on the procedure used to label the donor substrates, one or two minor DNAs of unknown structures that migrated more slowly than H-5 were also observed (lane 1). Each reaction mixture contained 2.1 μg of lysed viral protein. The left side identifies the various recombinants produced. The asterisk identifies an unknown DNA recombinant structure.

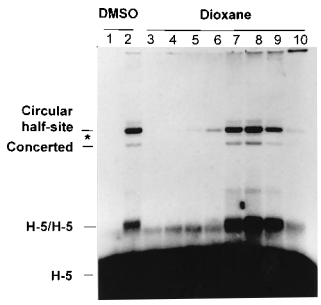

FIG. 5. Effect of aprotic solvents on the HIV-1 strand transfer reaction. Standard assay conditions were used, with 1.7 μg of virion protein per assay. The donor was H-5. The reaction time was 15 min. Lanes 1 and 3 contained no virus. Lane 2 contained 12% DMSO, and lane 3 contained 15% dioxane. Lanes 4 to 10 contained 0, 1, 5, 10, 15, 20, and 30% dioxane, respectively. The DNA products produced are shown on the left. The gel was exposed with a screen for 16 h.

are preset in the preincubation mixture prior to the strand transfer reaction (34, 35).

We also examined the influence that the donor-to-target ratio and protein concentration had on the circular half-site and the linear 3.8-kbp strand transfer reactions. The donor-to-target molar ratio was varied from 1 to 1 up to 4 to 1, respectively, at an optimal protein concentration (see below). The concentration of the pGEM target was held constant at 100 ng per reaction. The donor and target were preincubated together with IN on ice to increase the quantity of H-5–pGEM recombinants produced instead of having only the donor present during preincubation (Fig. 4). The total quantity of H-5–pGEM recombinants was increased approximately threefold between the lowest and highest donor-to-target ratios (data not shown). The linear 3.8-kbp and circular half-site H-5–pGEM recombinant reactions were equally affected. The optimal protein concentration was between 1.5 and 2.4 μg of virus lysate per reaction in reactions in which between 6 and 8% of the input donor was used for strand transfer reactions (data not shown). Increasing the quantity of virion lysate above these concentrations inhibited the donor-target reactions (Fig. 2).

DMSO and 1,4-dioxane were shown to significantly increase the strand transfer products that are produced with the M-2 donor and AMV IN (34, 35). Dioxane preferentially promoted (approximately sixfold) the formation of full-site M-2–pGEM recombinants over circular half-site recombinants compared with DMSO. The effects of DMSO and dioxane on the strand transfer reactions catalyzed by HIV-1 IN were investigated (Fig. 5). The NaCl concentration was increased to 60 mM in this experiment. Increasing the concentration of dioxane in the reaction mixture increased the amount of strand transfer products that were produced (Fig. 5, lanes 3 to 10). DMSO also stimulated the integration reaction in a manner similar to that of dioxane (Fig. 5, lane 2, and data not shown). However, the ratio of the concerted or linear 3.8-kbp products to the circular half-site products produced with 15% dioxane (Fig. 5, lane 8) was not significantly better than that observed with 12% DMSO (lane 2). These results suggest that although both aprotic solvents stimulated the strand transfer reactions in a manner similar to that of the avian integration system, dioxane does not preferentially enhance the HIV-1 IN concerted reaction as it does the AMV IN reaction.

PEG enhances the strand transfer reactions catalyzed by the murine leukemia virus, HIV-1, and Rous sarcoma virus nucleoprotein complexes isolated from virus-infected cells (2, 14, 24, 26) as well as with the purified AMV IN integration system (34, 35). Similar results were obtained with lysed HIV-1 virions and various concentrations of PEG. Standard assay conditions were employed. The maximum donor-donor, circular half-site, and linear 3.8-kbp strand transfer reactions were done with between 5 and 8% PEG (data not shown). These results suggest that volume-excluding reagents in general enhance the retrovirus integration reactions.

Kinetics of strand transfer, divalent metal ion requirements, and stability of preintegration complexes. The retroviral nucleoprotein complexes found in virus-infected cells (2, 3, 14, 17) and purified AMV IN (33–35) use Mg^{2+} for the 3′ OH trimming and full-site strand transfer reactions. Bacterially expressed IN uses only Mn^{2+} efficiently for the 3′ OH trimming and half-site strand transfer reactions (12, 31). HIV-1 IN in virion lysates effectively used Mg^{2+} for producing both the circular half-site and the concerted or linear 3.8-kbp products (Fig. 6). Mn^{2+} was less effective than Mg^{2+} for the linear 3.8-kbp reaction, but it was used efficiently for the circular half-site reaction (Fig. 6B). A lighter exposure of the gel in Fig. 6A showed that the H-5–H-5 recombinant reaction with Mn^{2+} was greater than the donor-donor reaction in the presence of Mg^{2+}. The H-5–pGEM reactions in the presence of either divalent metal ion were linear for approximately 15 min (Fig. 6A and B). *Bgl*II digestion of the pooled Mg^{2+} or Mn^{2+} reaction mixtures, as can be seen from Fig. 6A, demonstrated that both reaction mixtures produced the same H-5–pGEM recombinants but that the formation of the linear 3.8-kbp recombinants in the presence of Mn^{2+} was decreased (Fig. 6C). On the basis of the PhosphorImager analysis, it is clear that approximately 30% of the H-5–pGEM products from the pooled Mg^{2+} reactions migrated at the linear 3.8-kbp position, of which ~60% were due to concerted events (Table 1). The 3.8-kbp DNA produced with Mn^{2+} was not used to transform CA244 cells. A significant amount of the H-5–pGEM recombinant (denoted with asterisks in Fig. 6A and C) of an unknown structure was also produced in the Mg^{2+} reaction compared with that in the Mn^{2+} reaction. The data also show that Mg^{2+} is more efficiently used by the virion-derived IN than by the bacterially expressed HIV-1 IN (12) for both the circular half-site and the linear 3.8-kbp H-5–pGEM recombinant reactions.

We wanted to determine if Mg^{2+} was necessary for stabilizing the IN–H-5–pGEM complexes that were formed in the virus lysate. Also, it was important to understand how stable IN was in the preincubation mixture because proteases as well as nonspecific nucleases are associated with purified virus particles. The stability of the complexes was measured in the presence or absence of the divalent metal ion in the preincubation mixtures prior to catalysis (Fig. 7). A normal control reaction that included the standard preincubation step and the 15-min strand transfer reaction was also included (Fig. 7A, lane 2) and was quantitated in Fig. 7B. In the other control reactions, Mg^{2+} was always present, and the reactions were terminated by SDS treatment after various incubation periods at 2, 22, and 37°C (Fig. 7A, lanes 3, 5, 7, and 9). In the stability study, Mg^{2+} was added only after various times of preincubation at the indicated temperatures (Fig. 7A, lanes 4, 6, 8, and 10), which was followed by the normal 15-min strand transfer reaction. The entire H-5–pGEM populations for each reaction were quantitated, and the results are shown in Fig. 7B. The data suggest that Mg^{2+} was not absolutely necessary for maintaining the stability of IN–H-5–pGEM complexes prior to preincubation at 37°C. The nucleoprotein complexes were still relatively stable for 1 min at 37°C without Mg^{2+} (Fig. 7, lane 8) but were completely unstable upon preincubation for 5 min at this temperature without Mg^{2+} (lane 10). With other temper-

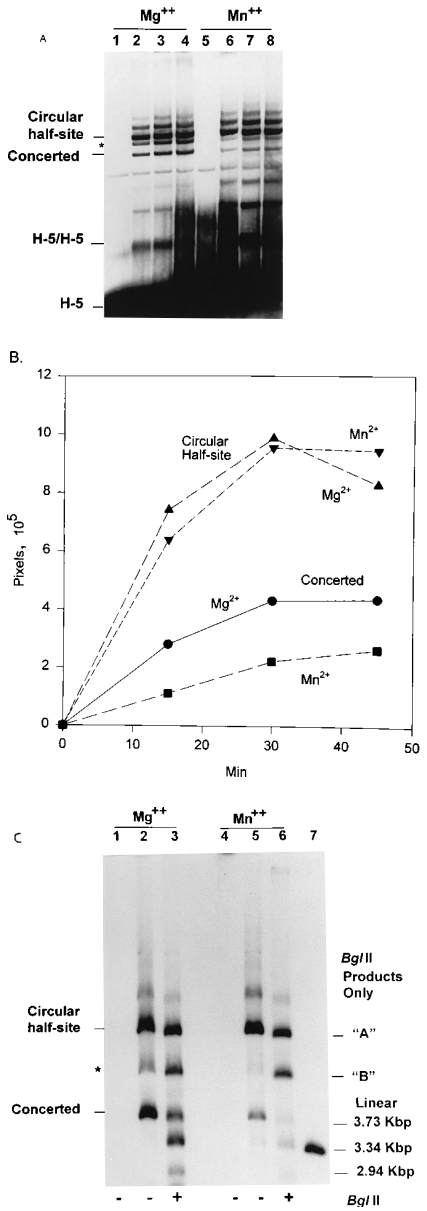

FIG. 6. Divalent metal ions affect the production of circular half-site and linear 3.8-kbp and concerted H-5–pGEM recombinants. (A) The integration efficiencies of H-5 into pGEM with Mg^{2+} and Mn^{2+} at 10 and 2 mM, respectively, were compared. H-5, pGEM, and IN were preincubated together under optimal 30 mM NaCl assay conditions. Lanes 1 and 5 lacked virus, while the other lanes each contained 1.7 μg of lysed virions. Lanes 2, 3, and 4 were incubated at 37°C for 15, 30, and 45 min, respectively. Lanes 6, 7, and 8 were incubated for the same lengths of times, respectively. The samples were processed and subjected to electrophoresis on a 1% agarose gel. The gel was dried and exposed to an X-ray film for 48 h without a screen. The top line indicates which divalent metal ions were present in the preincubation mixture. The left side shows the various recombinant products produced. (B) The dried gel shown in panel A was analyzed with a PhosphorImager. The circular half-site and concerted DNA products were quantitated for each time reaction and plotted as pixels against time. (C) Characterization of circular half-site and linear 3.8-kbp and concerted recombinants produced with either Mg^{2+} or Mn^{2+} by *Bgl*II digestion. One-half portions of each reaction mixture with Mg^{2+} and Mn^{2+} reported on in the legend to panel A were pooled and used for this analysis. Lanes 1 and 4 represent the negative control reactions. Lanes 2 and 5 represent one-half of each undigested reaction pool containing Mg^{2+} and Mn^{2+}, respectively. Lanes 3 and 6 contain the other half of the pools digested with *Bgl*II. The samples were subjected to electrophoresis on a 1.5% agarose gel. The dried gel was exposed for 8 h without a screen. Lane 7 contained a labeled 3.4-kbp linear DNA marker. The right side lists *Bgl*II digestion products, and the left side shows the undigested H-5–pGEM recombinants. The asterisk identifies the unknown recombinant.

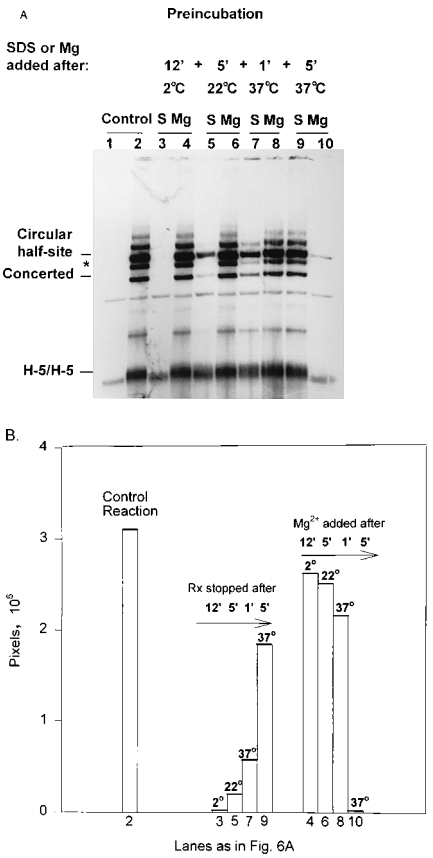

FIG. 7. Characterization of nucleoprotein complex formation and activity and stability of IN–H-5–pGEM recombinants after various preincubation times. Optimal 30 mM NaCl assay conditions were employed. Lane 1 contained no IN. All of the other lanes contained 2.1 μg of protein from lysed virions. Lane 2 was a control lane in which Mg^{2+} was present throughout the combined preincubation time of 17 min, which included 12 min at 2°C and 5 min at 22°C. Standard concentrations of H-5 and pGEM were used in the preincubation mixtures. The times and temperatures of each preincubation set which corresponded to the addition of SDS (S) or 10 mM Mg^{2+} (Mg) to each set are listed at the top. The SDS lanes contained Mg^{2+} prior to preincubation. After each continuous preincubation period, all of the strand transfer reactions were for 15 min at 37°C. The samples were terminated and subjected to electrophoresis on a 1% agarose gel. The dried gel was exposed for 45 h with a screen. The left side identifies the various recombinants produced. The asterisk identifies an unknown DNA recombinant structure. (B) The total quantities of all H-5–pGEM recombinants that were produced for each reaction (Rx) discussed in the legend to panel A were determined by PhosphorImager analysis. The results are plotted as pixels. The H-5–H-5 recombinants were not included in these analyses.

ature inactivation studies, the same results were obtained if 0.3 mM EDTA was also present in the preincubation mixture prior to the addition of 10 mM $MgCl_2$ to initiate strand transfer (Fig. 7B, lane 10, and data not shown).

DISCUSSION

The concerted integration of retrovirus-like DNA by IN derived from lysates of HIV-1 virions was accomplished. The integration reaction was analyzed by using 5′-end-labeled, 469-bp donor molecules and circular target DNA. Circular half-site and linear 3.8-kbp recombinants were separated on agarose gels and quantitated by PhosphorImager analysis. Sequence analysis of the linear 3.8-kbp DNA recombinants demonstrated that the HIV-1-specific, 5-bp host duplications had occurred (Table 1). A total of 55% of all recombinants had host site duplications of between 5 and 7 bp. In addition,

specific small deletions of between 17 and 51 bp that had a periodicity of ~10 bp were observed. These small deletions constituted 29% of all the linear 3.8-kbp recombinants. The order of the addition of donor or target molecules to the preincubation mixtures prior to strand transfer did not influence the ratio of linear 3.8-kbp products to circular half-site products that were produced.

The small deletions that were present in the linear 3.8-kbp DNA recombinants were produced by half-site integration events (Table 1). No deletions smaller than 17 bp were observed, and the deletions had a periodicity of ~10 bp, suggesting that some ordered event was occurring. Most of the small deletions were produced under low-salt lysis and assay conditions, although they were also present under high-salt lysis and strand transfer conditions. The mechanism involved in the formation of these small deletions is unknown. Possibly, IN is forming an oligomeric structure on the target, permitting the insertion of donors into pGEM at periodic locations along the oligomeric structure, or other viral or cellular proteins are directing IN-donor complexes to specific locations on the target. Only two deletions or two duplications mapped to the same site on pGEM (data not shown), suggesting that the DNA sequence was not the principal reason for the ordered events. It will be interesting to determine by sequence analysis whether the preincubation of target only (Fig. 4) instead of the donor-target together (Table 1) will enhance the formation of more deletions having a 10-bp periodicity compared with the 5- to 7-bp duplications.

The IN activity for our studies was derived from virus lysates of purified HIV-1 virions. The possibility that other viral proteins may influence the assembly of the nucleoprotein complexes containing IN as well as the strand transfer reactions exists. Although matrix, protease, reverse transcriptase, nucleocapsid, and contaminating cellular proteins including nucleases are present, the fidelity of the concerted integration reactions catalyzed by virion lysates was reasonably good (Table 1). In addition, the IN-donor-target complexes were relatively stable in the preincubation mixtures (Fig. 7).

On the basis of the assumption that IN constitutes 1% of the input protein (2 μg), our typical strand transfer reaction would contain 20 ng of IN. The concentration of IN would be 13 nM, and the ratio of IN dimer to H-5 ends would be approximately 1 to 1, respectively. Under optimal assay conditions of low salt and 12% DMSO (Fig. 4), approximately 7% of input H-5 was inserted into either other donor molecules or pGEM. These calculations suggest that although other proteins constitute the majority of the protein mass, IN was reasonably efficient in forming IN–H-5 complexes capable of producing the concerted recombinants or the specific deletions. Increasing the concentration of lysate above approximately 3 μg per assay caused an inhibition of strand transfer activity. The inhibition could be due to factors affecting the assembly of IN–H-5 and IN–H-5–pGEM complexes or to catalysis. Our results suggest that the physical assay will be useful for studying potential inhibitors of IN for both the half-site and full-site H-5–pGEM integration reactions.

There was no apparent precursor-product relationship between the unknown donor-target recombinant and any of the other DNA products (Fig. 6). Digestion of the unknown recombinant with *Bgl*II (Fig. 3, lanes 4 and 5) resulted in the production of the three linear products expected from *Bgl*II digestion of the linear 3.8-kbp DNA (Fig. 3, lanes 6 and 7). The data suggest that the unknown donor-target recombinant possesses a stable structure different from that of the linear 3.8-kbp DNA but contains the entire structure resulting from full-site events or adjacent insertions of two donors producing small deletions. The structure and sequence of this unknown recombinant population, which may contain more than one species, are under investigation.

What relationships exist between the HIV-1 IN systems (virion and bacterium expressed)? IN from bacteria can catalyze the 3′ OH trimming and half-site strand transfer reactions, using Mn^{2+} and oligonucleotides as donor substrates, with reasonable efficiency. The reason why expressed HIV-1 IN cannot effectively use Mg^{2+} for these reactions or perform the concerted strand transfer reactions is unknown. Recent studies using our standard H-5–pGEM strand transfer conditions have shown that bacterially expressed HIV-1 IN and HIV-2 IN can use Mg^{2+} fourfold more efficiently than they can use Mn^{2+} (data not shown). But only circular half-site and donor-donor products were produced in the presence of either divalent metal ion.

AMV IN (34, 35) has properties similar to those of virion HIV-1 IN, including the ability to use Mg^{2+} and to respond to both aprotic solvents used in this report. The virion proteins appear to require higher NaCl concentrations to produce full-site products. The optimal salt concentration for concerted integration with purified AMV IN is 0.35 M (34, 35), while HIV-1 IN required 300 mM for lysis and 60 mM for strand transfer (Table 1). Of the 44 sequenced avian recombinants isolated from the linear 3.8-kbp DNA, 37 of the recombinants had 5- to 7-bp host site duplications, with the avian 6-bp duplication predominating (34, 35). Several smaller duplications and one small deletion were produced by AMV IN. Whether the avian system under low-salt conditions produces small deletions with the periodicity observed in the HIV-1 system is presently being investigated.

ACKNOWLEDGMENTS

This work was supported by a National Institutes of Health grant (AI-31334).

We thank R. Inman for his analysis of the linear 3.8-kbp DNA by electron microscopy, S. Verma for helping with the DNA sequencing, and R. H. A. Plasterk and F. M. I. van den Ent for the purified HIV-1 and HIV-2 IN expressed in bacteria.

REFERENCES

1. **Bowerman, B., P. Brown, J. M. Bishop, and H. E. Varmus.** 1989. A nucleoprotein complex mediates the integration of retroviral DNA. Genes Devel. **3:**469–478.
2. **Brown, P. O., B. Bowerman, H. E. Varmus, and J. M. Bishop.** 1987. Correct integration of retroviral DNA in vitro. Cell **49:**347–356.
3. **Brown, P. O., B. Bowerman, H. E. Varmus, and J. M. Bishop.** 1989. Retroviral integration: structure of the initial covalent product and its precursor, and a role for the viral IN protein. Proc. Natl. Acad. Sci. USA **86:**2525–2529.
4. **Bukrinsky, M. I., S. Haggerty, M. P. Dempsey, N. Sharova, A. Adzhubel, L. Spitz, P. Lewis, D. Goldfarb, M. Emerman, and M. Stevenson.** 1993. A nuclear localization signal within HIV-1 matrix protein that governs infection of non-dividing cells. Nature (London) **365:**666–669.
5. **Bukrinsky, M. I., N. Sharova, M. P. Dempsey, T. L. Stanwick, A. G. Bukrinskaya, S. Haggerty, and M. Stevenson.** 1992. Active nuclear import of human immunodeficiency virus type 1 preintegration complexes. Proc. Natl. Acad. Sci. USA **89:**6580–6584.
6. **Bukrinsky, M. I., N. Sharova, T. L. McDonald, T. Pushkarskaya, G. Tarpley, and M. Stevenson.** 1993. Association of integrase, matrix, and reverse transcriptase antigens of human immunodeficiency virus type 1 with viral nucleic acids following acute infection. Proc. Natl. Acad. Sci. USA **90:**6125–6129.
7. **Bushman, F. D., and R. Craigie.** 1991. Activities of human immunodeficiency virus (HIV) integration protein *in vitro*: specific cleavage and integration of HIV DNA. Proc. Natl. Acad. Sci. USA **88:**1339–1343.
8. **Bushman, F. D., T. Fujiwara, and R. Craigie.** 1990. Retroviral DNA integration directed by HIV integration protein in vitro. Science **249:**1555–1558.
9. **Chow, S. A., and P. O. Brown.** 1994. Substrate features important for recognition and catalysis by human immunodeficiency virus type 1 integrase identified by using novel DNA substrates. J. Virol. **68:**3896–3907.
10. **Craigie, R., T. Fujiwara, and F. D. Bushman.** 1990. The IN protein of Moloney murine leukemia virus processes the viral DNA ends and accomplishes their integration in vitro. Cell **62:**829–837.

11. **Ellison, V., and P. O. Brown.** 1994. A stable complex between integrase and viral DNA ends mediates human immunodeficiency virus integration *in vitro*. Proc. Natl. Acad. Sci. USA **91:**7316–7320.
12. **Engelman, A., F. D. Bushman, and R. Craigie.** 1993. Identification of discrete functional domains of HIV-1 integrase and their organization within an active multimeric complex. EMBO J. **12:**3269–3275.
13. **Engelman, A., K. Mizuuchi, and R. Craigie.** 1991. HIV-1 DNA integration mechanism of viral DNA cleavage and DNA strand transfer. Cell **67:**1211–1221.
14. **Farnet, C. M., and W. A. Haseltine.** 1990. Integration of human immunodeficiency virus type 1 DNA *in vitro*. Proc. Natl. Acad. Sci. USA **87:**4164–4168.
15. **Farnet, C. M., and W. A. Haseltine.** 1991. Determination of viral proteins present in the human immunodeficiency virus type 1 preintegration complex. J. Virol. **65:**1910–1915.
16. **Fitzgerald, M. L., A. C. Vora, W. G. Zeh, and D. P. Grandgenett.** 1992. Concerted integration of viral DNA termini by purified avian myeloblastosis virus integrase. J. Virol. **66:**6257–6263.
17. **Fujiwara, T., and K. Mizuuchi.** 1988. Retroviral DNA integration: structure of an integration intermediate. Cell **54:**497–504.
18. **Goff, S. P.** 1992. Genetics of retroviral integration. Annu. Rev. Genet. **26:** 527–544.
19. **Grandgenett, D. P., R. B. Inman, A. C. Vora, and M. L. Fitzgerald.** 1993. Comparison of DNA binding and integration half-site selection by avian myeloblastosis virus integrase. J. Virol. **67:**2628–2636.
20. **Gulizia, J., M. P. Dempsey, N. Sharova, M. I. Bukrinsky, L. Spitz, D. Goldfarb, and M. Stevenson.** 1994. Reduced nuclear import of human immunodeficiency virus type 1 preintegration complexes in the presence of a prototypic nuclear targeting signal. J. Virol. **68:**2021–2025.
21. **Heinzinger, N. K., M. I. Bukrinsky, S. A. Haggerty, A. M. Ragland, V. Kewalramani, M. Lee, H. E. Gendelman, L. Ratner, M. Stevenson, and M. Emerman.** 1994. The Vpr protein of human immunodeficiency virus type 1 influences nuclear localization of viral nucleic acids in nondividing cells. Proc. Natl. Acad. Sci. USA **91:**7311–7315.
22. **Katz, R. A., G. Merkel, J. Kulkosky, J. Leis, and A. M. Skalka.** 1990. The avian retroviral IN protein is both necessary and sufficient for integrative recombination in vitro. Cell **63:**87–95.
23. **Katzman, M., R. A. Katz, A. M. Skalka, and J. Leis.** 1989. The avian retroviral integration protein cleaves the terminal sequences of linear viral DNA at the in vivo sites of integration. J. Virol. **63:**5319–5327.
24. **Kitamura, Y., Y. M. Lee, and J. M. Coffin.** 1992. Nonrandom integration of retroviral DNA in vitro: effect of CpG methylation. Proc. Natl. Acad. Sci. USA **89:**5532–5536.
25. **LaFemina, R. L., C. L. Schneider, H. L. Robbins, P. L. Callahan, K. LeGrow, E. Roth, and W. A. Emini.** 1992. Requirement of active human immunodeficiency virus type 1 integrase enzyme for productive infection of human T-lymphoid cells. J. Virol. **66:**7414–7419.
26. **Lee, Y. M., and J. M. Coffin.** 1991. Relationship of avian retrovirus DNA synthesis to integration in vitro. Mol. Cell. Biol. **11:**1419–1430.
27. **Roe, T., T. C. Reynolds, G. Yu, and P. O. Brown.** 1993. Integration of murine leukemia virus DNA depends on mitosis. EMBO J. **12:**2099–2108.
28. **Sherman, P. A., and J. A. Fyfe.** 1990. Human immunodeficiency virus integration protein expressed in Escherichia coli possesses selective DNA cleaving activity. Proc. Natl. Acad. Sci. USA **87:**5119–5123.
29. **Stevenson, M., S. Haggerty, C. A. Lamonica, C. M. Meier, S. K. Welch, and A. J. Wasiak.** 1990. Integration is not necessary for expression of human immunodeficiency virus type 1 protein products. J. Virol. **64:**2421–2425.
30. **Vink, C., and R. H. A. Plasterk.** 1993. The human immunodeficiency virus integrase protein. Trends Genet. **9:**433–437.
31. **Vink, C., K. H. van der Linden, and R. H. A. Plasterk.** 1994. Activities of the feline immunodeficiency virus integrase protein produced in *Escherichia coli*. J. Virol. **68:**1468–1474.
32. **Vink, C., D. C. van Gent, Y. Elgersma, and R. H. A. Plasterk.** 1991. Human immunodeficiency virus integrase protein requires a subterminal position of its viral DNA recognition sequence for efficient cleavage. J. Virol. **65:**4636–4644.
33. **Vora, A. C., M. L. Fitzgerald, and D. P. Grandgenett.** 1990. Removal of 3′-OH-terminal nucleotides from blunt-ended long terminal repeat termini by the avian retrovirus integration protein. J. Virol. **64:**5656–5659.
34. **Vora, A. C., and D. P. Grandgenett.** Assembly and catalytic properties of retrovirus integrase-DNA complexes capable of efficiently performing concerted integration. Submitted for publication.
35. **Vora, A. C., M. McCord, M. L. Fitzgerald, R. B. Inman, and D. P. Grandgenett.** 1994. Efficient concerted integration of retrovirus-like DNA in vitro by avian myeloblastosis virus integrase. Nucleic Acids Res. **22:**4454–4461.